A STUDY ON DEVELOPING OF EPOXY/POSS NANOCOMPOSITE AND TO INVESTIGATE THEIR THERMO–MECHANICAL BEHAVIOR

By

KUNAL MISHRA

Bachelor of Technology in Mechanical Engineering
Uttar Pradesh Technical University
Lucknow, UP, India
2008

Submitted to the Faculty of the
Graduate College of
Oklahoma State University
in partial fulfillment of
the requirements for
the Degree of
MASTER OF SCIENCE
May, 2011

A STUDY ON DEVELOPING OF EPOXY/POSS NANOCOMPOSITE AND TO INVESTIGATE THEIR THERMO–MECHANICAL BEHAVIOR

Thesis Approved:

Dr. Raman P. Singh

Thesis Advisor

Dr. Ali K. Kalkan

Dr. Kevin Ausman

Dr. Mark Payton

Dean of the Graduate College

ACKNOWLEDGMENTS

I am heartily thankful to my advisor, Dr. Singh, whose encouragement, supervision and support from the preliminary to the concluding level enabled me to develop an understanding of the subject. It would have been next to impossible to work on research and write this thesis without Dr. Singh support.

I would like to thanks Dr. Kalkan and Dr. Ausman for there precious time and support throughout my research work.

I would like to thanks Gajendra sir for his continuous cooperation in each and every step. He was always there with his helping hand whenever I felt the need of his expertise. Also I would like to thanks Seshumani for her guidance and help in chemistry related part.

My roommates and lab mates Jain, Suman and Bhadra ji helped me and supported me always in thick and thin phase of OSU. Also I want to show gratitude to my lab members Leila, Arif, Austin, Mohammed, Phil, Matt, Chirag, Dhivakar, Balaji, Vasudevan, Chaitanya, and Nawani sir for there support and patience to bear me. I would like to thanks Krishna and Lawanya for there valuable help in chemistry related topics and experiments.

At last I am thankful to my parents, sisters and Ankita who always encouraged and cooperated with me at all stages of my life.

TABLE OF CONTENTS

LIST OF TABLES

Table Page

LIST OF FIGURES

CHAPTER 1

INTRODUCTION

Tonnes of epoxy resins and their respective hardeners are produced each year. These epoxy resins are used in various applications like adhesive, coating, and are also used as matrix in fiber-reinforced composites, compared to thermoplastic polymers. These cured resins have superior mechanical properties that include high glass transition temperature, high modulus, creep resistance, low shrinkage at elevated temperature and good resistance against chemicals. These properties of epoxy based resin resulted from a high degree of chemical cross-linking given by diglycidyl ether of bisphenols. Nonetheless these products also tend to be brittle due to high cross-linking density and therefore are usually brittle and vulnerable to fracture. [1, 2]

In recent years, a considerable amount of work has been done in an attempt to enhance the properties of these resins, by reinforcing of a second phase in the epoxy resin. Different reinforcement fillers of different kinds such as rubber particles [3–9], thermoplastics [10], metal particles [11–17], silicate layer [18–27], ceramic particles [28], glass beads [29, 30], carbon nanofibers [31–35], carbon nanotubes (CNT) [36–40], and combination of two fillers [34, 41] have been used previously with some success.

With the addition of these fillers in resin, there is a change in the curing kinetics, local stoichiometry, curing reaction and, curing temperature of neat resin. As a consequence of these changes, there is a change in the mechanical properties of a filler reinforced matrix, which is accounted by variation in cross-linking of polymer in presence of particles and

also local physical interactions near the particle surface [42].

Conventionally, epoxy resins have been reinforced with micron-sized fillers. Micron sized particles tend to form agglomerates easily at low percentage loading. These agglomerates may induce stress concentration, which initiates cracks and make them larger than the critical crack size that causes failure. Since past years, there has been a lot of research going on in developing nano sized particles. These are particles of size between 1-100 nanometers. In most of cases the effect of fillers in resin decrease with the increase in size. Various researches have shown that compared to micro sized fillers, nano fillers have some unique properties, like interfacial area between matrix and filler. In the nano–filler scenario, due to high density of particles per volume (typically 10^6–10^8 particles/mm^3), promotes stress transfer from soft matrix to hard nano particles leading to increased strength and stiffness of the composite. As a result of this only small amounts of fillers are needed to cause significant changes. Also nano sized filler show uniform dispersion and avoidance of agglomeration in polymer compared to micron–sized fillers [42, 43].

Mechanical properties of filler reinforced resins can be enhanced by a variety of energy dissipative mechanisms. These mechanisms are dependent on different variables including the chemical nature of filler, filler size, and filler loading. In case of toughening with organic matters like rubber particles and thermoplastics, energy is dissipated in the plastic zone near the crack through shear yielding process. Unfortunately, use of such organic matter decreases the modulus of the resin system. When inorganic particles with high modulus are used as fillers toughening is seen to occur via various mechanisms of energy dissipation without compromising the modulus. Examples of such mechanisms includes crack pinning, crack bridging, crack path deflection, and micro cracking. However, inorganic particles bundle up easily forming agglomerates at low loadings results in deterioration of epoxy resin properties. So in order to get a better dispersion of the nano filler in matrix

researchers have tried several techniques which in turn increase the preparation and fabrication time as well as make procedure complicated.

In past some years, due to the development of organic-inorganic hybrid nano composites, researcher showed great interest in this hybrid nano composites [44–47]. As they combine advantages of the inorganic materials (rigidity, high stability) and the organic polymers (flexibility, reactivity and processebility). Polyhedral oligomeric silsesquioxane (POSS) is the kind of hybrid material that possess both organic and inorganic properties, having a size between 1–3 nm. POSS is made up of organic–inorganic monomer silsesquioxane ($RSiO_{1.5}$). Figure 1.1 shows schematic of POSS.

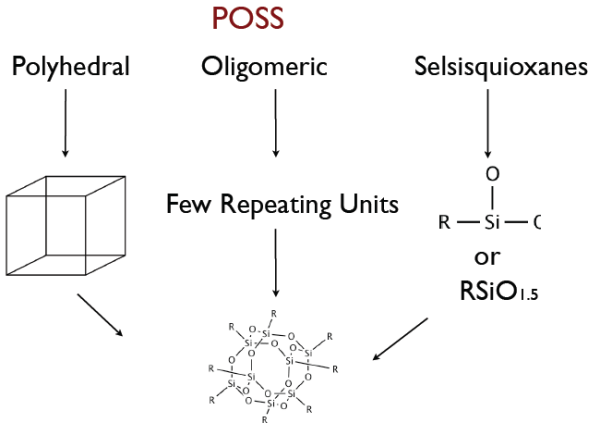

Figure 1.1: General schematic of formation of POSS (Polyhedral oligomeric silsesquioxane).

The formula of POSS is $(SiO_{1.5})_8R_8$, possess inorganic rigid cage type structure containing silicon and oxygen where organic group (R) attached to silicon. Figure 1.2 shows molecular structure of POSS. POSS can be reactive or non reactive and it can interact with epoxy resin in two ways:

1. Reactive organic substituents of POSS react with polymer chain forming covalent bonds.

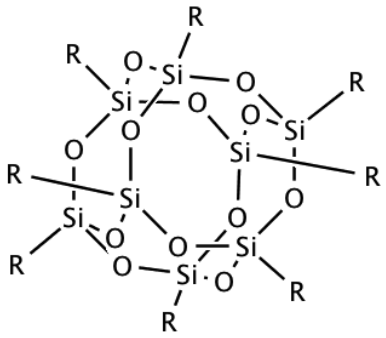

Figure 1.2: Molecular structure of general POSS structure, POSS possess inorganic cage structure with organic substituent attached on silicon atom.

2. Shows compatibility either by similarities in chemical structure or by specific polar interaction between non reactive organic substituent of POSS and polymer chain.

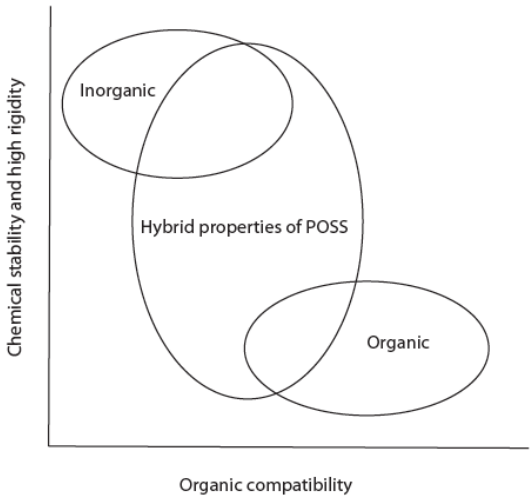

Figure 1.3: POSS possess unique organic–inorganic properties. Organic substituent provide compatibility and reactivity while inorganic cage provides rigidity and stability in nano composite.

Reactive organic part gives processibility and reactivity while rigid inorganic cage part gives stability in epoxy/POSS nano composite. Dispersion of POSS in epoxy resin is dependent on interaction of organic substituent of POSS with polymer. POSS can be dispersed at molecular level depending on, kind of the reaction between POSS and polymer

and in micro level due to excellent compatibility of POSS and polymer. Usually, positive reinforcement is obtained if there is good interaction between polymer and POSS.This dual nature of POSS along with the fact that it is a nano sized filler validates its selection as a filler for epoxy resins, as we have seen that perviously [56].

Lot of work has done till date on reinforcing of POSS, such as investigating formation of nanoscale structure [48], synthesizing novel POSS [49–54, 68], investigating mechanical properties [**?**, 55–60, 67, 71], synthesis with other nanofiller like clay [61] to enhance physical properties like thermal degradatation [62–64, 69], and glass transition [65].

Focus of this study is to develop and synthesis epoxy/POSS nanocomposites using simple technique with better dispersion of nano filler and to characterize these nanocomposites in terms of mechanical, chemical and physical properties.

CHAPTER 2

MATERIAL PREPARATION

2.0.1 Materials

The two types of composite matrix analyzed in this work are (i) EPON 862 (Hexion speciality chemicals, Columbus, OH), a diglycidyl ether of bisphenol F based resin cured with curing agent Epikure 3274, a low viscosity aliphatic amine and (ii) SC79 Part A (Applied poleramics, Benificia, CA) a diglycidyl ether of bisphenol A based resin cured with curing agent SC79 Part B, a cylcoaliphatic amine.

The reason behind selecting these epoxy resins was their superior mechanical properties, chemical resistance, and ease of fabrication. Also these resin systems have been very well studied in literature. Figure 2.1 shows the molecular structure of diglycidyl ether of bisphenol F and aliphatic amine used.

Figure 2.2 shows the molecular structure of diglycidyl ether of bisphenol A and cy-

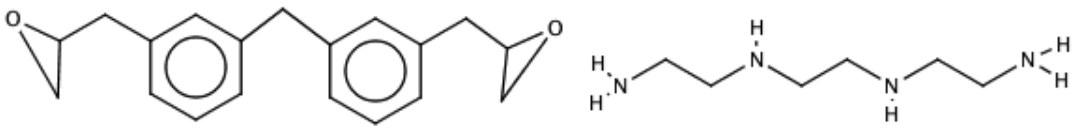

(a) DGEB-F (EPON 862) (b) triethylene tetraamine (Epikure3274)

Figure 2.1: Molecular structure of (a) Diglycidyl ether of bisphenol F and (b) aliphatic amine used as hardener. DGEB–F is the major constituent of EPON 862 that provide high cross–linking density.

cloaliphatic amine used.

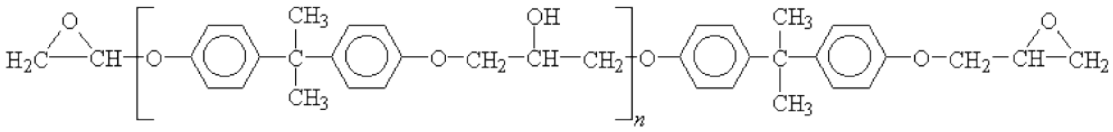

(a) DGEB-A (SC79)

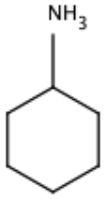

(b) Monomer of cyclo aliphatic amine

Figure 2.2: Molecular structure of (a) Diglycidyl ether of bisphenol A and (b)cycloaliphatic amine used as hardener. DGEB-A is the major constituent of SC79 part A.

	Epon 862 [74]	SC79–Part A [73]
Manufacturer	Hexion co. ltd.	Applied Poleramics
Curing agent	Epikure 3274	SC79–Part B
Curing cycle	24 h at 25°C; 6 h at 121°C	5 h at 121°C
Fracture toughness	1.1 MPam$^{1/2}$	1.1 MPam$^{1/2}$
Density	1.17gm/cc	1.16 gm/cc

Table 2.1: Properties of epoxy resins used for this work.

Property	Trisilanol phenyl	Methacryl	Glicidyl[[75]
Resin solubility	Most aliphatic and aromatic , monomers, oligomers, polymers	Aliphatic, aromatic and epoxy resin	Aliphatic, aromatic, and epoxy resin
Appearance	White powder	Clear to hazy, colorless oil	Viscous liquid.
Density	1.42 gm/cc	1.25 gm/cc	1.24 gm/cc

Table 2.2: Properties of different functionality of POSS

For diglycidyl ether of bisphenol–F, three different functionalities of POSS were used namely, trisilanol phenyl, methacryl, and glycidyl POSS while for diglycidyl ether of bisphenol–A, methacryl and glycidyl POSS were used. These POSS were purchased from Hybrid Plastics, Hattiesburg, MS. Figure 2.3 shows molecular structure of these POSS. The reason behind selecting these POSS is their interaction with the epoxy resins as discussed in introduction. Manufactured properties of POSS are shown in Table 2.2.

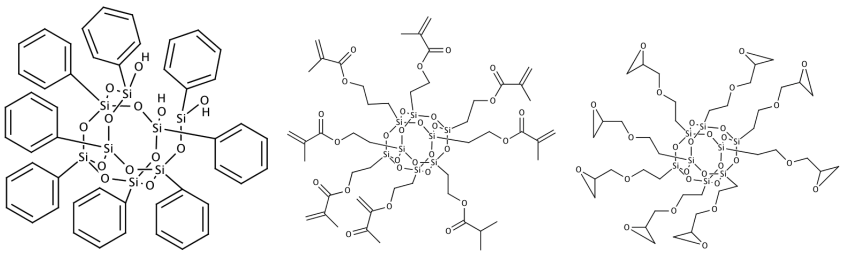

Figure 2.3: Molecular structure of (a) Trisilanol phenyl, (b) Methacryl, and (c) Glycidyl POSS, these three kinds of POSS selected according to functional group present on silicon atom.

2.0.2 Sample preparation

DGEB–F

Epoxy resin was mechanically mixed with all three functionalities of POSS overnight at 50 °C and continuously stirred at 400 rpm. The mixture was then left at room temperature for cooling till it reached ambient temperature.

Curing agent (Epkiure 3274) added to this mixture in the ratio of 100 parts of epoxy resin

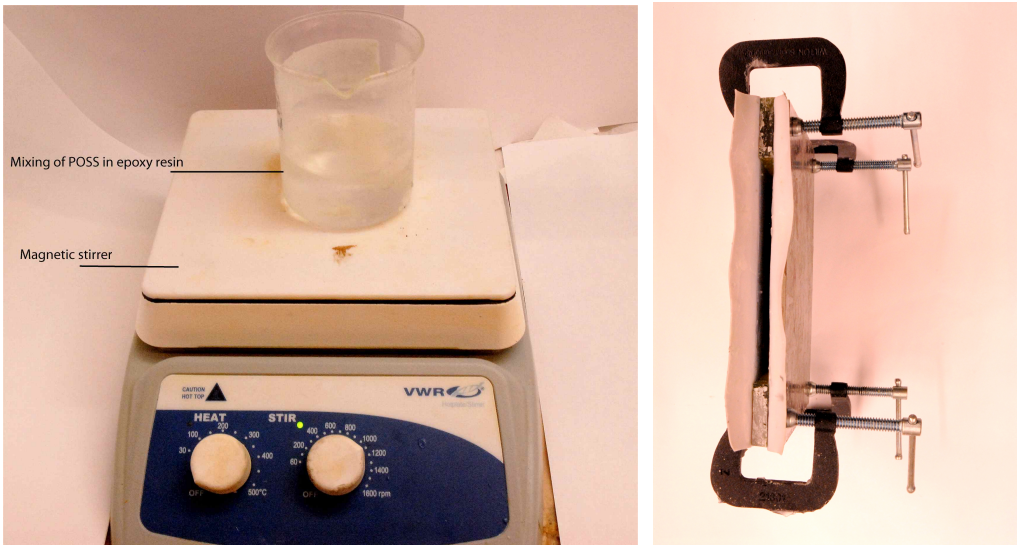

Figure 2.4: Molecular structure of (a) Mixing of POSS in epoxy resin at 50 °C, (b) Pre prepared mold in which POSS-epoxy mixture poured.

to 40 parts by wt. % of curing agent. This ternary mixture was then mechanically mixed at room temperature for 10 minutes at 400 rpm. The mixture was then placed in a vacuum chamber for 30 minutes for degassing, in order to remove gas bubbles that were introduced during mixing. Finally, the mixture was poured into a pre-prepared mold (fig. 2.4 (b)) and was cured at room temperature for 24 hours. Then, the casted resin plate was taken out from mold and put into curing oven for post curing at 121 °C (250 °F) for 6 hours. The same curing cycle was used for preparing neat resin as a baseline material.

DGEB–A

Epoxy resin was mechanically mixed with POSS overnight using magnetic stirrer at 50 °C and continuously stirred at 400 rpm. The mixture was then left at room temperature for cooling, followed by the addition of curing agent in ratio of 100 parts of epoxy resin to 40 parts of curing agent by weight. This was then mixed using magnetic stirrer at room temperature for 10 minutes at 400 rpm. The mixture was then placed in a vacuum chamber for 30 minutes for degassing, in order to remove the gas bubbles that were introduced during mixing. Finally, the mixture was poured into a pre-prepared mold and let it cured at 121°C in a curing oven for three hours.

CHAPTER 3

CHARACTERIZATION

3.0.3 Fracture toughness determination

Fracture toughness was determined using single edge notch bend test as per the ASTM D–5045 on universal testing machine (Instron 5567, Norwood, MA). The sample was machined from cast plate in series of 54.00mm x 12.70mm x 6.35mm. [77] A 4.5mm deep

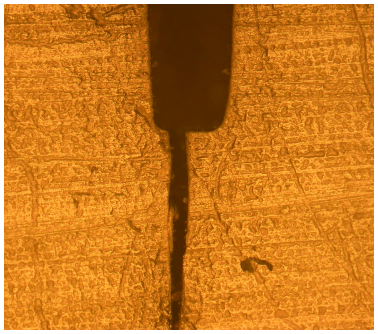

Figure 3.1: Optical image of notch specimen with pre–crack.

notch was cut using a diamond precision saw, and then the tip of the notch was tapped with a fresh razor blade using a hammer, to initiate a natural pre-crack as shown in fig. 3.1. For each case, 5–6 samples were tested. The pre–crack single edge notch specimen was loaded under three point bending test until failure. Tests were performed in a displacement–controlled mode at a fixed cross head speed of 0.5 mm/min. Figure 3.2 shows single edge notch specimen under three point bend test The fracture toughness of nano composites was measured in term of critical stress intensity factor (K_{Ic}) calculated by equation 3.1.

$$K_{Ic} = \frac{P}{B\sqrt{W}} f(\frac{a}{W}) \tag{3.1}$$

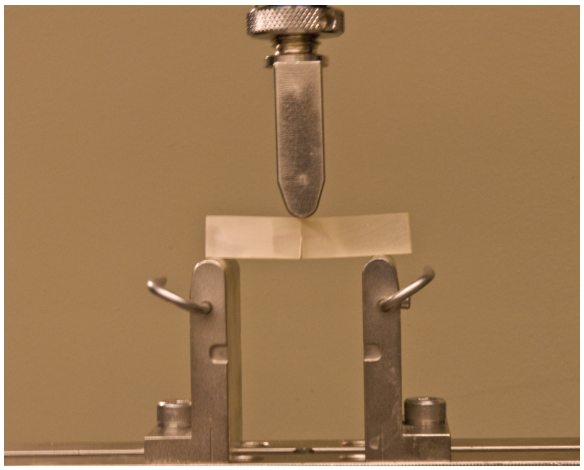

Figure 3.2: Three point bend testing of single edge notch beam specimen at 0.5mm/min.

where P is the maximum applied force, B is the thickness of specimen, W is width of the specimen and f is geometry factor given by equation 3.2.

$$f(\frac{a}{W}) = \frac{3\frac{S}{W}\sqrt{\frac{a}{W}}}{2(1+2\frac{a}{W})(1-\frac{a}{W})^{3/2}} \times [1.99 - (\frac{a}{W})(1-\frac{a}{W})(2.15 - 3.93\frac{a}{W} + 2.7(\frac{a}{W})^2)] \quad (3.2)$$

3.0.4 Flexural modulus and strength determination

Flexural modulus and strength was determined using three point bend rest according to ASTM D790 on universal testing machine. The sample was machined from cast plate in a series of 110.00mm x 25.40mm x 6.35mm. [78] The specimen loaded under the three point bending test until failure. Tests were performed in a displacement–controlled mode at a fixed cross head speed calculated by equation 3.4, according to ASTM standard.

$$R = \frac{ZL^2}{6d} \quad (3.3)$$

where Z = 0.01, L is span length and d is thickness. The flexural strength is calculated by following equation.

$$\sigma_f = \frac{3PL}{2bd^2} \quad (3.4)$$

Where P is the maximum load bear by the specimen. Modulus of elasticity is calculated by following equation.

$$E_b = \frac{PL^3}{4bd^3m} \tag{3.5}$$

Where m is the slope, obtained from the load displacement graph from raw data in three point bend test.

3.0.5 Fourier transform infrared spectroscopy (FTIR)

FTIR spectroscopy measurements were performed using FTIR spectrometer (Nicolet iS10, Waltham, MA) using 128 scans at a resolution of 2.0 cm^{-1}. Each spectrum was recorded from 4000 to 500 cm^{-1} at room temperature. Spectra were analyzed using a window-based software Ominic 5.1. The specimen was finely powdered using grinder, before collecting spectra.

3.0.6 Scanning electron microscopy

The surface morphology of the fractured surface was studied using Scanning electron microscope SEM microscope (Hitachi S-4800 FESEM, Dallas, TX). The samples were sputtered upto 50nm by gold on Crissington sputter coater, before microscopy to make them conductive.

3.0.7 Differential scanning calorimetry(DSC)

Thermal analysis of samples was carried out using a Q 2000 DSC (TA instruments, Inc.). After calibration with high purity indium, samples weighed around 5-10mg was placed on the DSC cell and then heated at scan rate of 10°C/min within the range -10°C to 210°C. Then, the specimen was instantaneously cooled to -10°C using liquid nitrogen after the first scan. The second scan was then performed in similar a way. The obtained data is extracted from second heating.

3.0.8 Density measurement

Density measurement was carried out for neat resin (both DGEB–A and DGEB–F) and epoxy/POSS nanocomposites. The three different ways used for calculating density, were;

1. Using rules of mixture (ρ_a).

2. Using Archimedese principal to find bulk density (ρ_b), which is, given as

$$\frac{\text{density of object}}{\text{density of fluid}} = \frac{\text{weight of object}}{\text{weight of object- apparent immersed weight}}. \tag{3.6}$$

3. Using pycnometer to find solid density (ρ_c).

CHAPTER 4

RESULT AND DISCUSSION

4.0.9 Fracture toughness

DGEB–F

The critical stress intensity factor as a function of POSS loading on DGEB–F resins are showed in fig.4.1. From the graph 4.1, we can observe that with incorporation of POSS

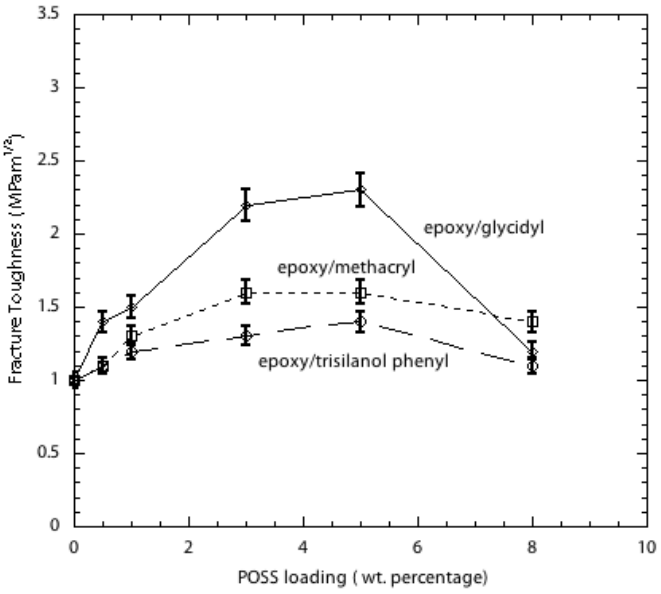

Figure 4.1: Fracture toughness value in terms of critical stress intensity factor (K_{Ic}) for different loading of POSS of different functional group.

in neat resin, K_{Ic} increase linearly with loading of POSS till 5 %wt. after that fracture toughness value starts decreasing. This pattern is same for all three functionality of POSS. Especially in case of epoxy/gylcidyl POSS nanocomposite, K_{Ic} increased by 2.3 times for 5 %wt. of POSS. While i of epoxy/methacryl and epoxy/trisilanolphenyl nanocomposite

showed an increase of K_{Ic} by 1.4 and 1.6 times of neat resin respectively. The statistical spread of experimental data is denoted by the error bars in terms of the standard deviation. A comparison is made between the load–displacement curve from raw data for neat resin and epoxy/POSS nano composites of similar crack length. Figure 4.2 shows the load–displacement curves for neat epoxy and epoxy/POSS. Neat resin, epoxy/methacryl, and epoxy/trisilanol phenyl exhibits brittle failure mode whereas epoxy/glycidyl nano composite shows ductile failure mode.

From load–displacement graph we can also conclude that epoxy/glycidyl composite fails at higher load than other epoxy/POSS nanocomposites as well as neat resin. This supports the fracture toughness value obtained in fig. 4.1. To estimate the work done during the failure of specimens under the single edge notch bend testing, the area under the curve was calculated as well as fractured area measured under optical microscope. The work of fracture computed and plotted using equation 4.1.

Also, the fracture surfaces areas were measured under an optical microscope equipped

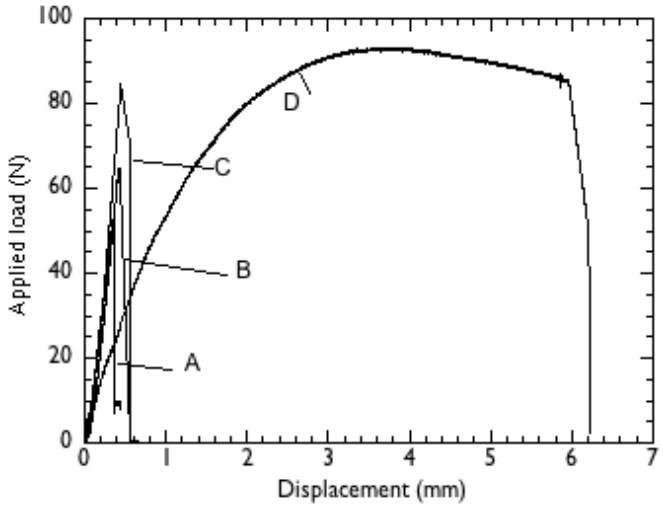

Figure 4.2: Load displacement curve for, (A) Neat resin, (B) Epoxy with trisilanol phenyl POSS, (C) Epoxy with methacryl POSS, and (D) Epoxy with glycidyl POSS.

with a micrometer stage. The work of fracture calculated was directly from the formula.

$$\text{Work of fracture} = \frac{\text{area under load displacement curve}}{2 \times \text{ area of fracture}} \tag{4.1}$$

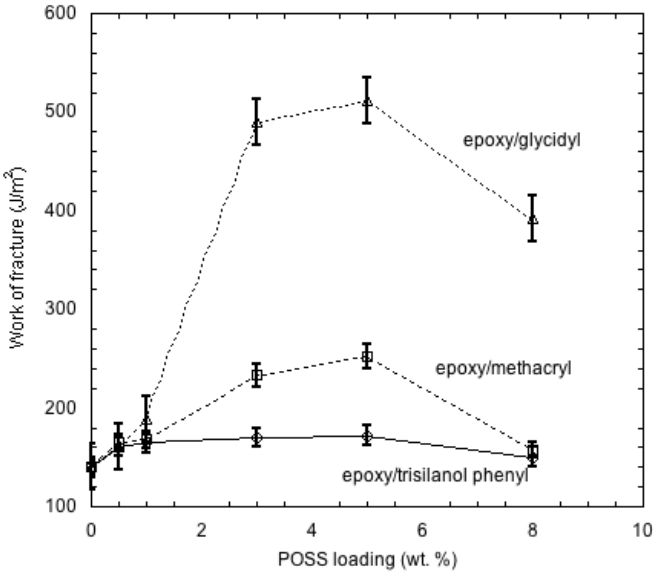

Figure 4.3: Work of fracture for neat resin and POSS incorporated resin.

Figure 4.3 shows the value of work of fracture obtained using equation 4.1. It shows that energy dissipating in crack initiation and propagation is more in POSS reinforced epoxy than neat resin. In case of glycidyl POSS reinforced epoxy, the energy dissipating is much higher than any other epoxy/POSS nanocomposites which indicates the higher fracture toughness and extensive plastic deformation of epoxy/glycidyl composites. Work done on fracturing epoxy/glycidyl composites is three times higher than that of neat resin. It is postulated that this high value of work of fracture is due to the combination of fracturing of specimen and plasticization near crack tip. In fig. 4.4, high stress concentration can be observed near crack tip, this may be due to plasticization of epoxy/glycidyl POSS nano composite.

In order to observe the ductility behavior change by loading of glycidyl POSS on epoxy resin, load–displacement curve of different wt. % of epoxy/glycidyl POSS is plotted as shown in fig.4.5. From the graph we observe that below 3 wt. % loading epoxy/glycidyl composite shows brittle failure while above that it shows transition from brittle to ductile failure. At higher percentage of POSS loading, the mechanical properties of epoxy/glycidyl

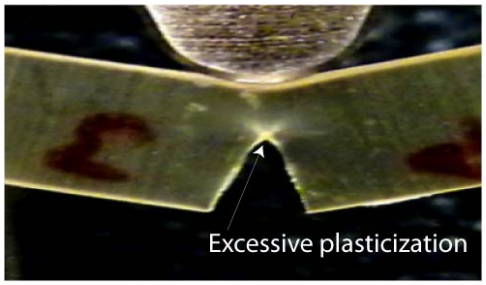

Figure 4.4: High stress concentration at the crack front of 5 wt. % epoxy/glycidyl nano composite.

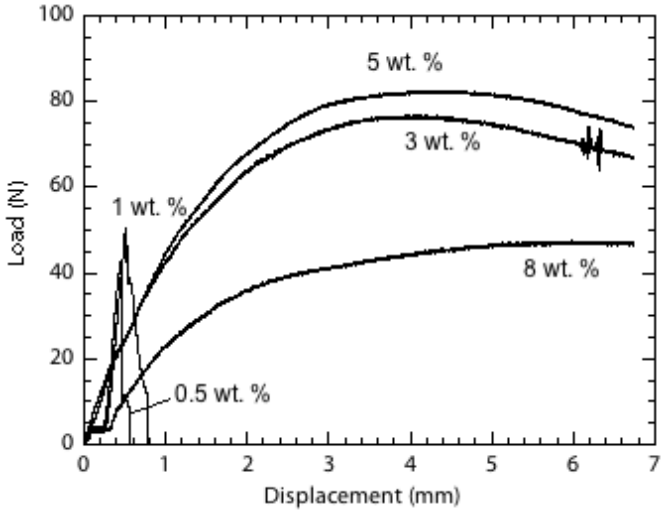

Figure 4.5: Load displacement curve for different percentage of glycidyl POSS reinforced epoxy resin.

composite degrade its properties, which may be due to formation of aggregates.

DGEB–A

The critical stress intensity factor as a function of POSS loading on DGEB–A is shown in fig. 4.6. K_{Ic} value for POSS incorporated resin, first increases with loading then attains a

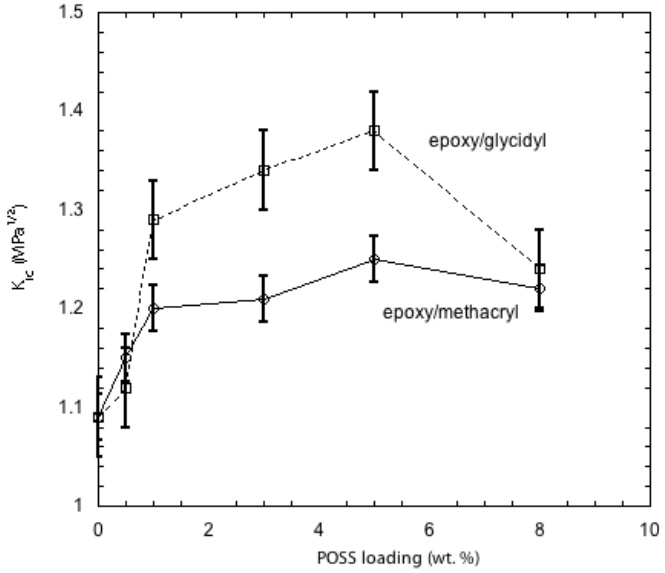

Figure 4.6: Fracture toughness comparison for DGEB–A resin.

maximum peak after which it starts decreasing. This pattern is same for both POSS, in case of epoxy/glycidyl nano composite it shows maximum value of 1.4 times higher than that of neat resin at 5 wt.% while epoxy/methacryl nano composite shows maximum value of 1.2 times higher than that of neat resin. Experimental scattering showed in terms of standard deviations.

Same as DGEB–F resin, load–displacement curve is plotted for neat DGEB–A resin and POSS incorporated resin having same crack length. Figure 4.7 shows that epoxy/glycidyl composite bear higher load than epoxy/methacryl composite and neat resin. Neat resin and epoxy/POSS composites show brittle mode of failure. In order to understand work done in fracturing of specimen, work of fracture was computed using eq. 4.1, following the same

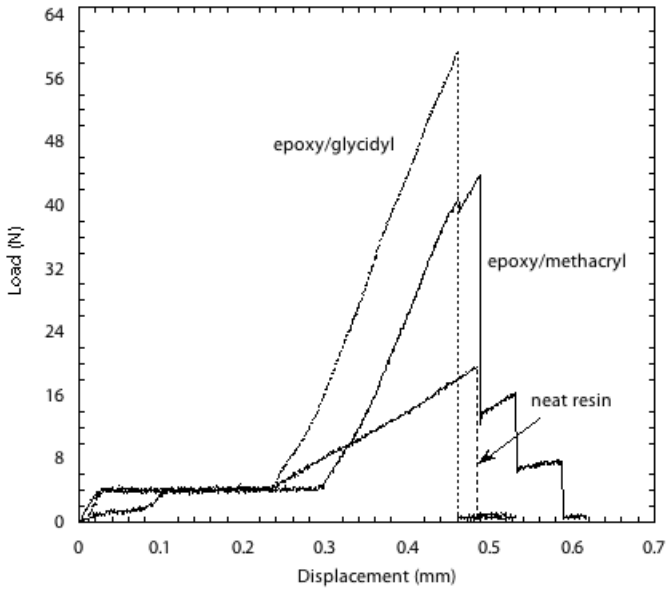

Figure 4.7: Load displacement curve for neat resin, and epoxy/POSS nano composite.

procedure in case of DGEB–F resin. Figure 4.8 shows work done in failure of specimen, we can observe from graph that work done for fracturing epoxy/glycidyl POSS is 1.5 times higher than that of neat resin.

4.0.10 Flexural strength and modulus of elasticity

DGEB–F

The modulus of elasticity and flexural strength is obtained by three point bend test as shown in fig. 4.9. We observe that, epoxy/methacryl and epoxy/trisilanol phenyl composites do not exhibit much change in value of flexural strength and modulus as there is large scatter in data while in case of epoxy/glycidyl flexural strength increases then decreases and modulus continuously decreases.

It has been noted from the values of fracture toughness, flexural strength, flexural modulus, load–displacement curve for different percentage of loading of glycidyl POSS that below 1 wt. % of loading, epoxy/glycidyl nano composite shows brittle failure but on increasing

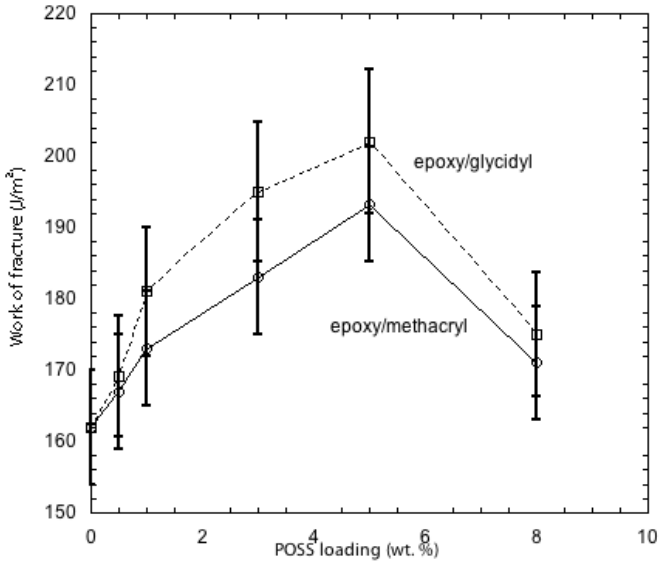

Figure 4.8: Work of fracture for neat resin, and epoxy/POSS nano composite.

the amount of POSS content epoxy/glycidyl nano composite changes its failure mode from brittle to ductile.

DGEB–A

Figure 4.10 shows that flexural strength of epoxy/POSS nano composites does not vary as compared to neat resin as there is large scatter in data, except epoxy/glycidyl nano composites. In order to understand mechanism and chemical interaction between POSS and polymer resin fourier transformation infra red spectroscopy was performed.

4.0.11 FTIR analysis

DGEB–F

The Fourier transform infrared spectroscopy was used to examine the degree of curing after the POSS cages were introduced to the systems and also the interaction between the POSS molecules and the epoxy systems. Shown in fig. 4.11 are the FTIR spectra of epoxy

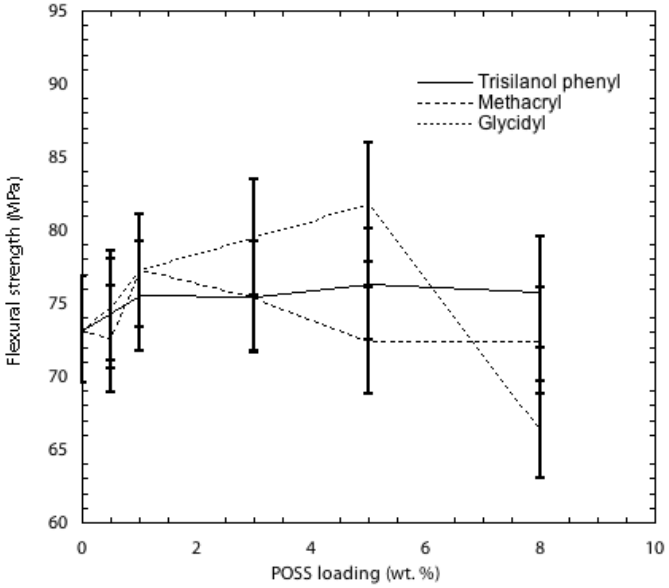

(a) Flexural strength

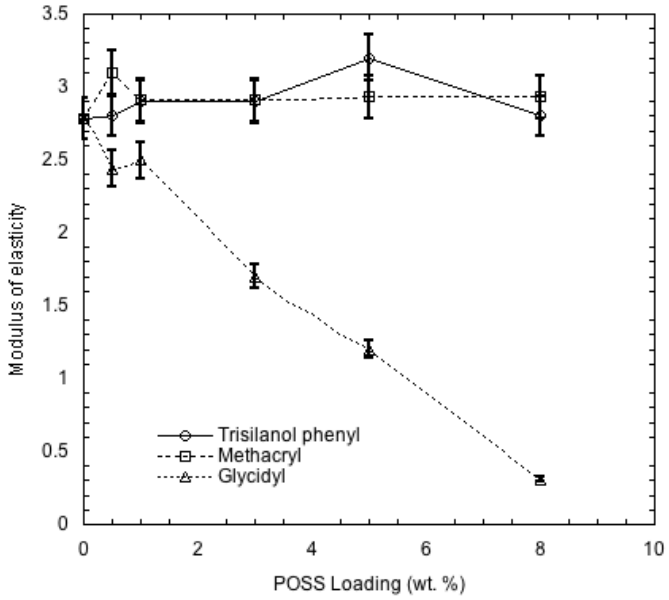

(b) Modulus of elasticity

Figure 4.9: (a) Flexural strength and (b) Modulus of elasticity for DGEB–F resin, epoxy/POSS nano composite do not show much change in value considering large scattering in data.

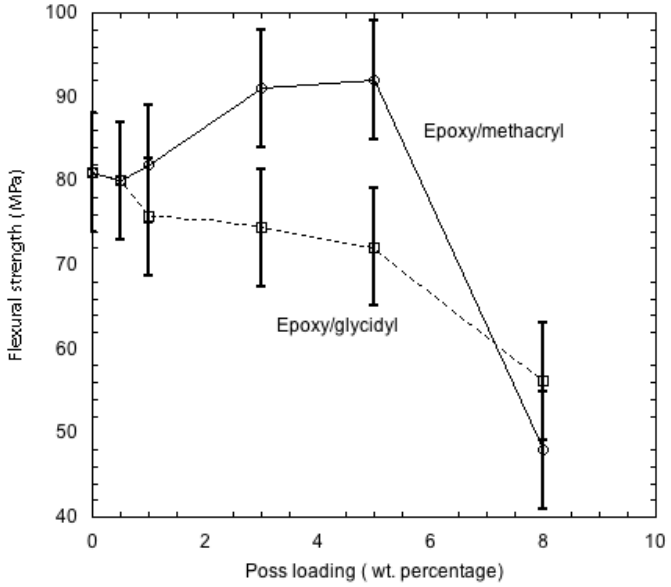

(a) Flexural strength

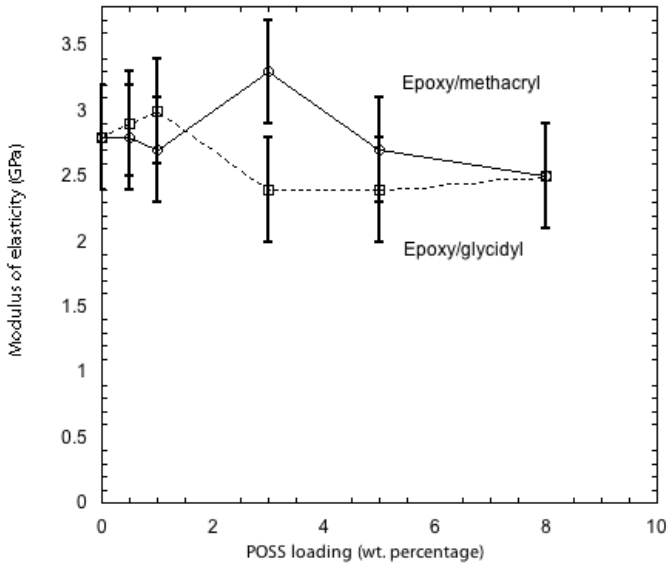

(b) Modulus of elasticity

Figure 4.10: (a) Flexural strength and (b) Modulus of elasticity for DGEB–A resin.

alone as the control and the nanocomposites containing 5 %wt. of POSS. The pure epoxy is characterized by the stretching vibration band of epoxide groups at 915 cm^{-1}.

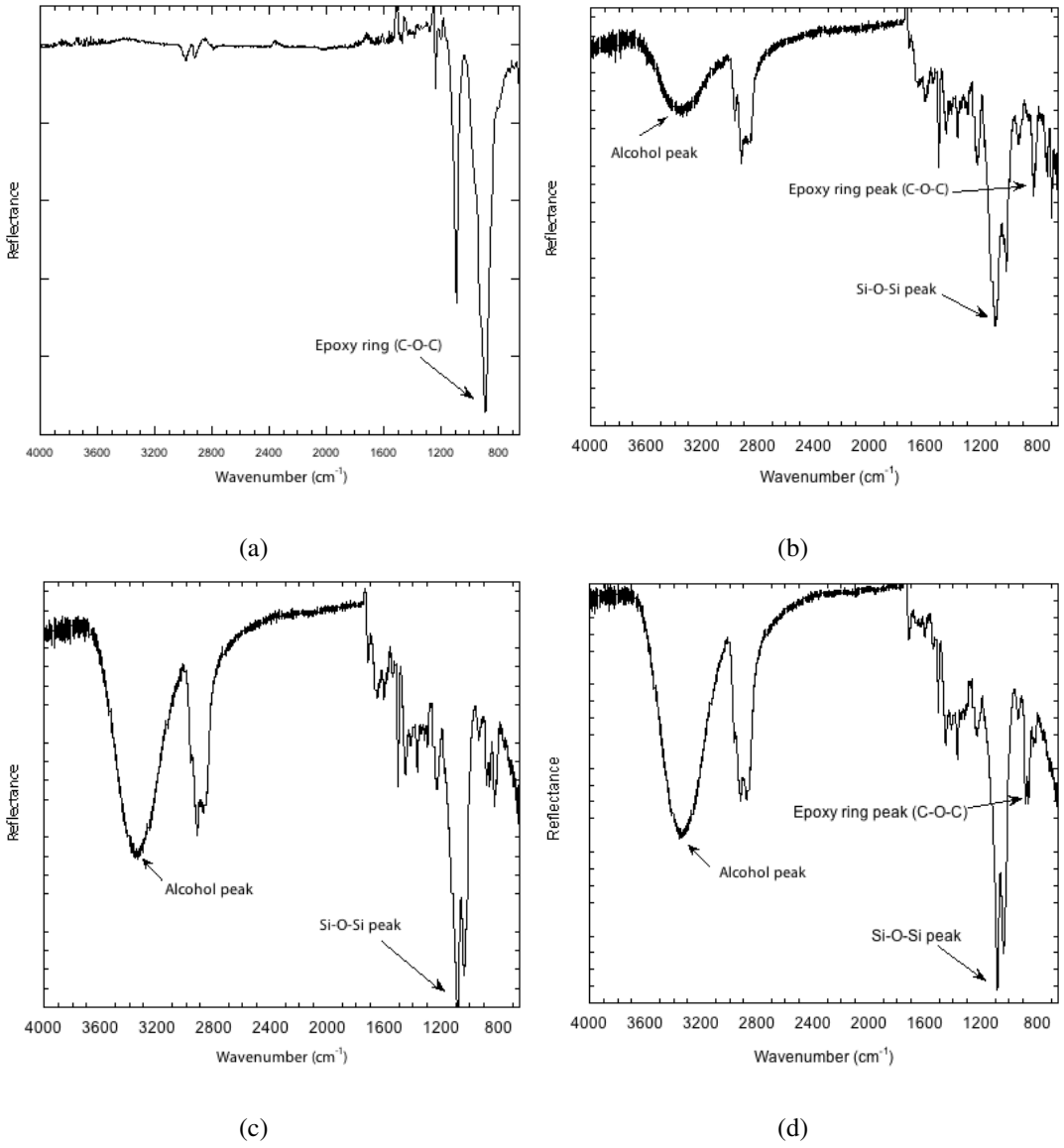

Figure 4.11: Spectra of (a) Neat resin (b) Epoxy/trisilanol phenyl nanocomposite (c) Epoxy/methacryl nanocomposite and (d) epoxy/glycidyl nanocomposite.

In case of epoxy/trisilanol nanocomposites, the peak at 901cm^{-1} indicates presence of epoxy ring but it is slightly shifted during polymerization. It means trisilanol phenyl

POSS only interact with the POSS without reacting with epoxy resin. While in case of epoxy/methacryl nanocomposites epoxy ring at 915 cm^{-1} is vanished also broad peak of alcohol around (3500–3200 cm^{-1}) shows occurrence of polymerization. Epoxy/glycidyl nanocomposites shows presence of epoxy ring around 912 cm^{-1} which may be due to un-cured epoxy ring from POSS or polymer resin, it also shows Si-O-Si network peak around 1024 cm^{-1} which shows POSS consumed by epoxy resin.

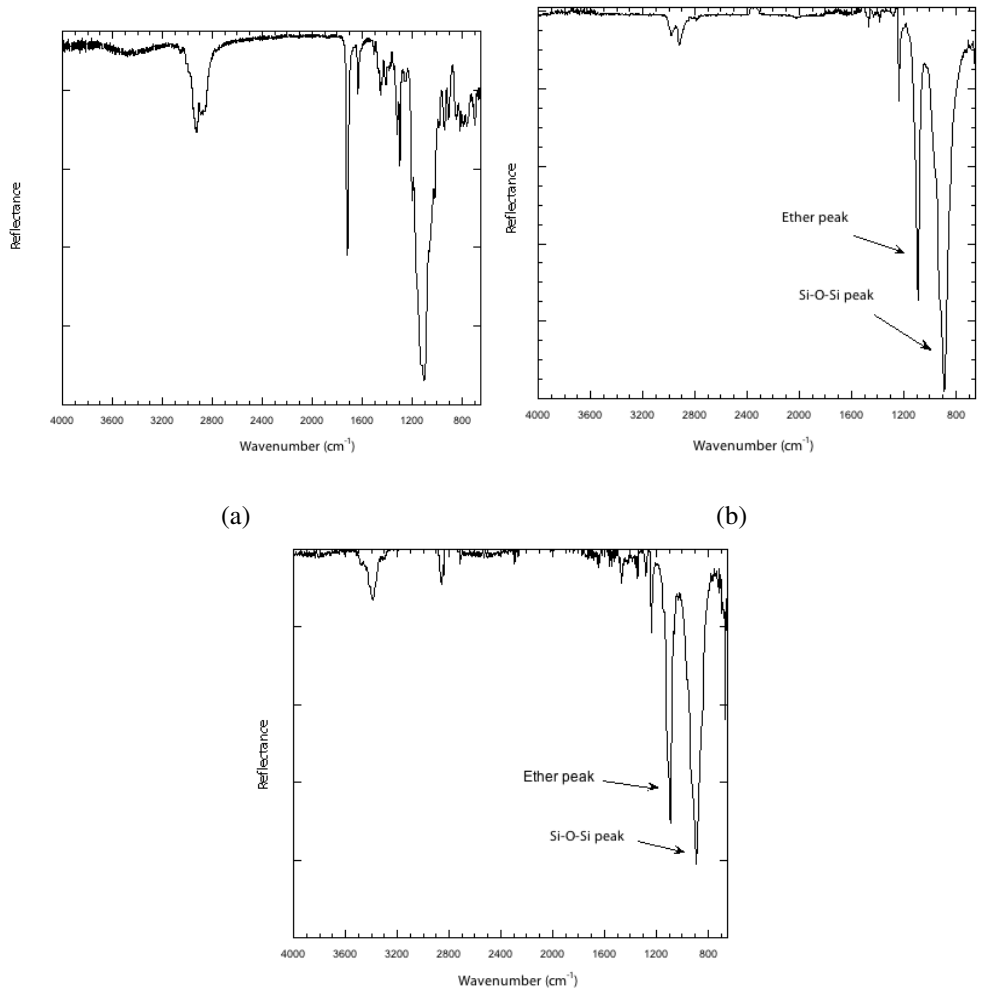

Figure 4.12: Spectra of (a) Neat resin (b) Epoxy/methacryl nanocomposite and (c) Epoxy/glycidyl nanocomposite.

From FTIR spectroscopy of DGEB–F resin and POSS incorporated resin, it can be concluded that trisilanol phenyl POSS is not reacting completely with resin. Methacryl POSS shows good reaction between POSS and epoxy resin as epoxy ring is vanished. Glycidyl POSS shows uncured epoxy ring, which indicates glycidyl POSS reacting with epoxy resin but not curing completely.

DGEBA–A

In case of DGEB–A based nanocomposites there is not much change in spectra between neat resin and POSS reinforced nanocomposites as shown in fig.4.12, which may be due to the steric hindrance due to two pendant methyl group present in it.

4.0.12 DSC thermogram analysis

DGEB–F

The DSC thermograms obtained for DGEB–F resin and 5 wt. % epoxy/POSS nanocomposites are shown in fig.4.13. A step corresponding to glass transition is visible in the temperature range 35°C to 50° C. It can be observed that with addition of nano filler the position of T_g shifted either at higher or lower temperature. This phenomena of decreasing value of T_g depends on the type and degree of interaction of POSS with polymer.

DGEB–A

The DSC thermograms obtained for DGEB–A resin and POSS reinforced epoxy are shown in fig. 4.14. A step corresponding to glass transition is visible in the temperature range of 150 °C to 190 °C. It can be observed that with the increase in loading of nano filler, the position of the T_g peak is shifted towards lower temperature. Such decrease in T_g, however,

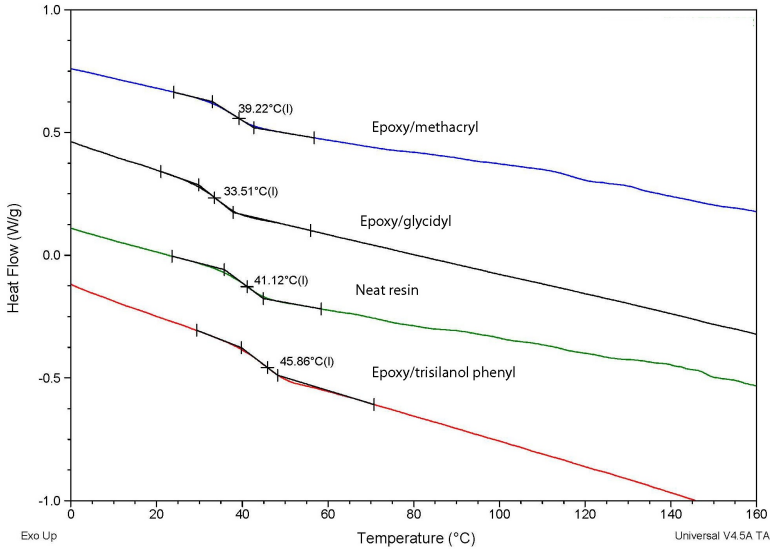

Figure 4.13: DSC thermogram for neat resin and 5 %wt. POSS incorporated resin.

was not fully linear, but being relatively greater importance for low POSS contents. With respect to the neat resin the 3% methacryl and glycidyl samples showed a drop in temperature by 18 °C and 30 °C, respectively whereas a drop of about 13 °C and 21° at 8 wt. % for epoxy/methacryl and epoxy/glycidyl POSS respectively.

As described previously in introduction, POSS can interact with polymer in two ways. Either functional group of POSS can react with polymer chain or due to the compatibility of functional group of POSS and polymer chain. Hence POSS can react with polymer chain followed by merging in polymer chain increasing polymer free volume and cause decrease of T_g. Figure 4.15 shows mechanism of interaction of organic part of POSS with polymer chain.

This decrease in T_g can be attributed plasticization effect. So depending on the POSS nature (i.e organic substituent present) and degree of dispersion, POSS can acts as a plasticizer (increasing free polymer volume). In case of epoxy/trisilanol phenyl composite, phenyl part of trisilanol phenyl POSS shows compatibility with phenyl part of polymer chain, so POSS restricts the mobility of chain and thus increases T_g (in case of DGEB–F resin).

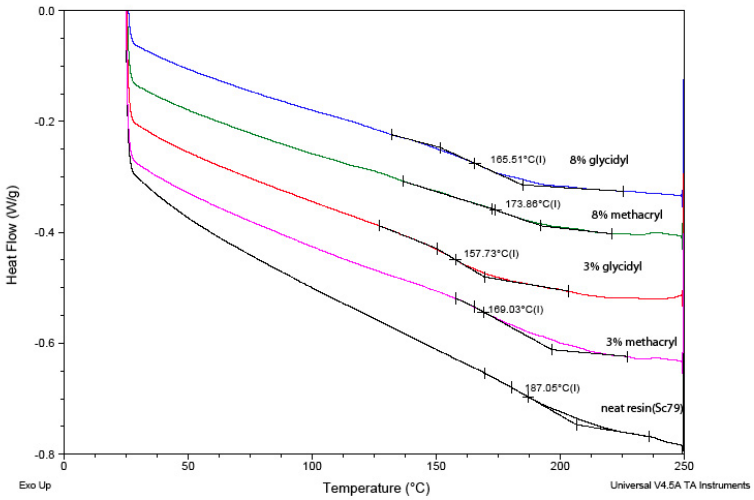

Figure 4.14: DSC thermogram for neat resin, 3 wt. %, and 5 wt. % POSS incorporated resin.

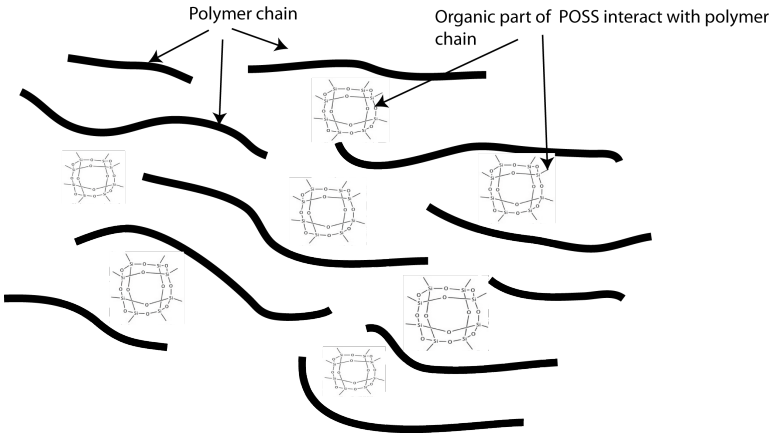

Figure 4.15: Schematic nanostructure model of POSS in Epoxy molecular network.

In case of epoxy/glycidyl and epoxy/methacryl, organic part of POSS group react with polymer chain, so that POSS stitches to polymer chain merging with it, which increase the free volume and decrease the glass transition. This continuous decrease in T_g signals plasticization of specimen prominently in case of epoxy/glycidyl composite in which glycidyl POSS react with polymer chain also shows compatibility due to similar glycidyl structure in POSS and in resin. We saw effect of plasticization in case of glycidyl POSS reinforced epoxy, as it shows decrease in flexural modulus [42, 56].

4.0.13 Fractography

To characterize the failure behavior in detail SEM was used. SEM micrographs of fractured surface are shown in fig. 4.16 for DGEB–F resin and POSS reinforced resin. It has been observed that for neat epoxy fractured surfaces are smooth except some scratches on surface, whereas in case of POSS reinforced epoxy the surfaces are comparatively rough. These rough surfaces dissipate high energy during crack propagation, which was calculated as work of fracture. This indicated the lower fracture resistance of neat epoxy resin compared to POSS reinforced resin system.

Epoxy/methacryl nanocomposites at higher magnification (fig. 4.17), shows the formation of craters and size of these craters increases with POSS loading, these craters could be void which formed due to debonding of POSS molecule from nanocomposite. As their size is increases with increase in the amount of POSS which indicated which indicated the formation of agglomeration at higher percentage. While in case of epoxy/glycidyl nanocomposite at higher magnification (fig 4.18) we can see the formation of microcracks, which increases with increasing the amount of POSS. Epoxy/glycidyl shows toughening by microcracking and also by crack pinning as we observe in jumping of crack.

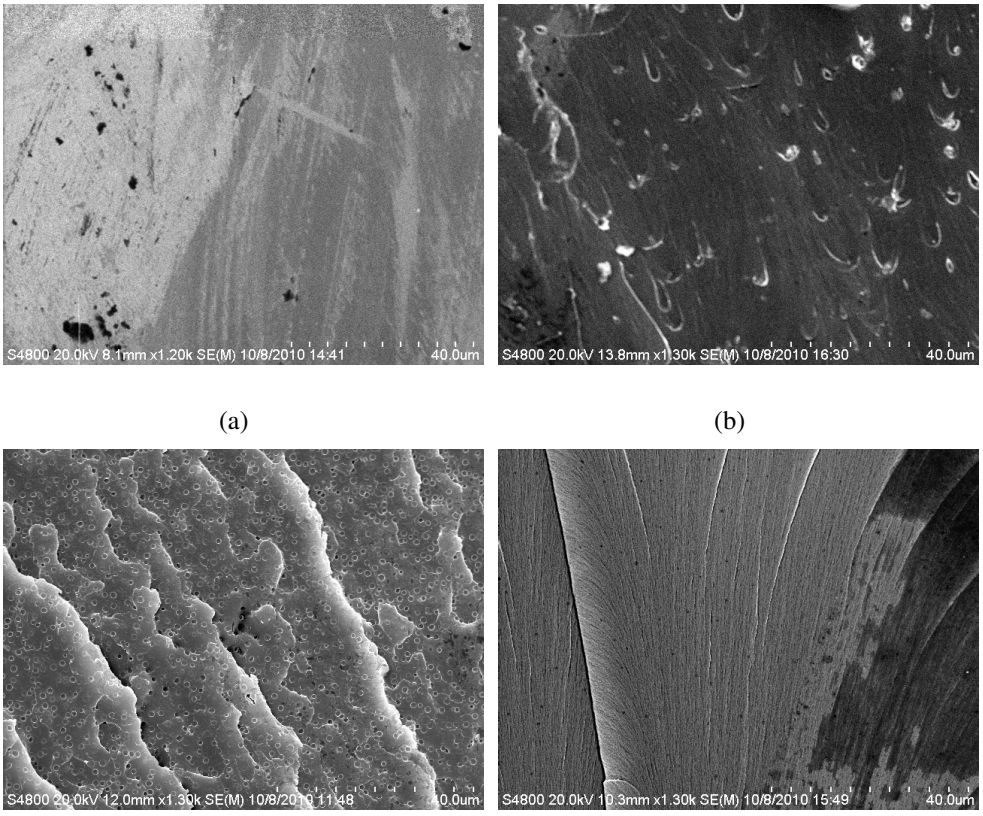

Figure 4.16: Electron microscopy of fractured image of (a) DGEB–F resin (b) epoxy/trisilanol phenyl nanocomposite (c) epoxy/methacryl nanocomposite and (d)epoxy/glycidyl nanocomposite.

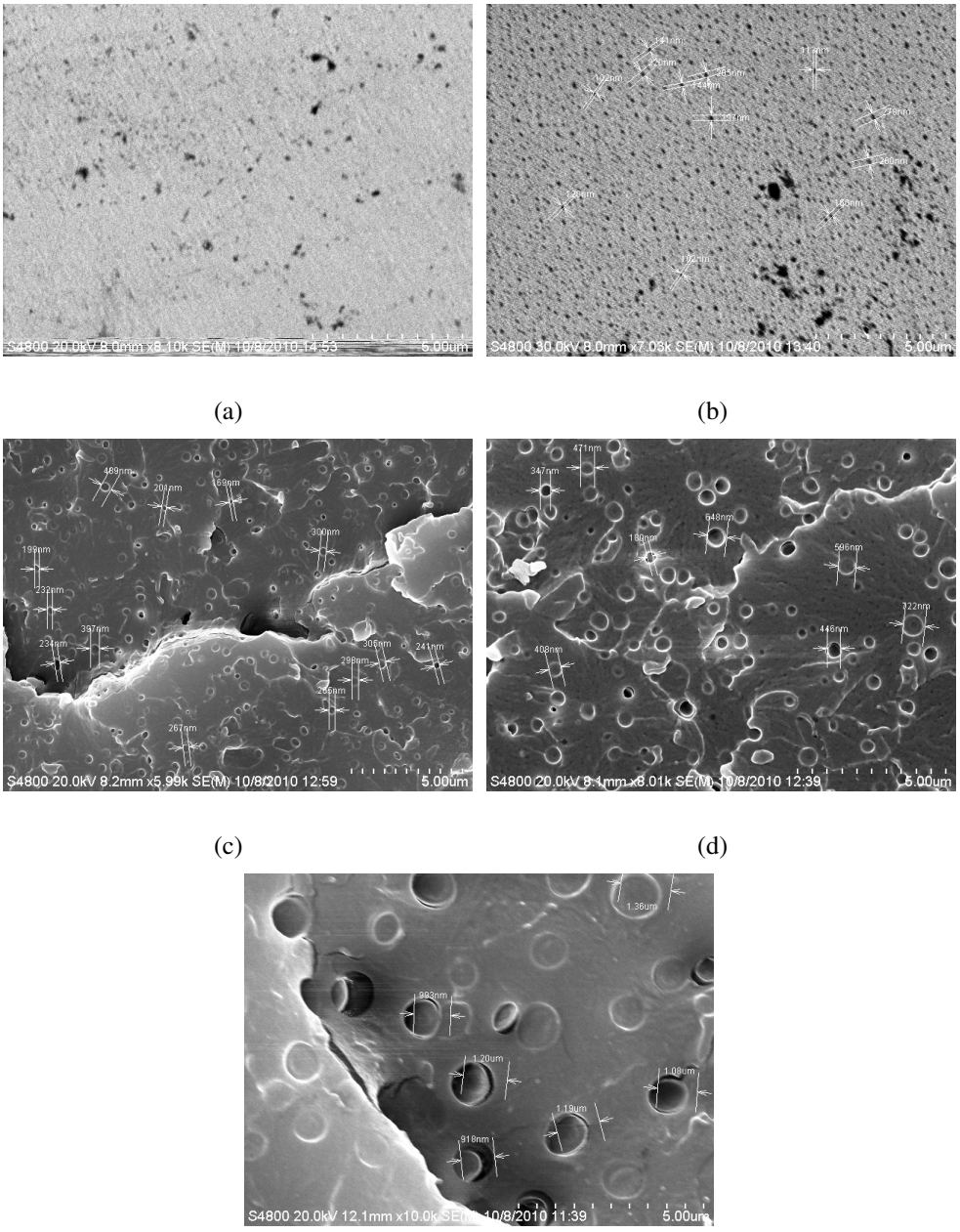

(a) (b)

(c) (d)

(e)

Figure 4.17: Scanning electron microscopy of fractured image of epoxy/methacryl nanocomposite at (a)0.5%, (b) 1% (c) 3%, (d) 5% and (e) 8% loading.

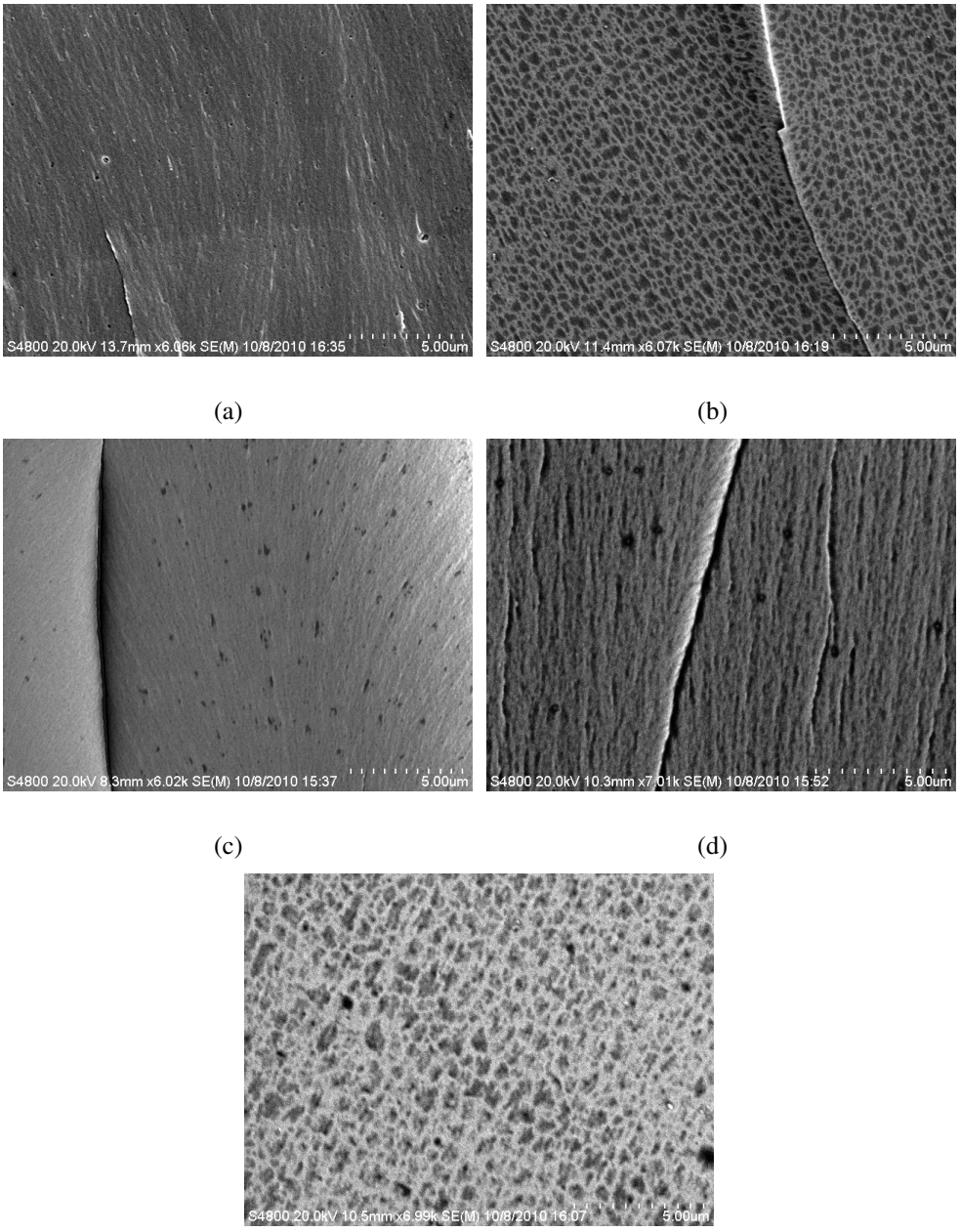

Figure 4.18: Scanning electron microscopy of fractured image of epoxy/glycidyl nanocomposite at (a)0.5%, (b) 1% (c) 3%, (d) 5% and (e) 8% loading.

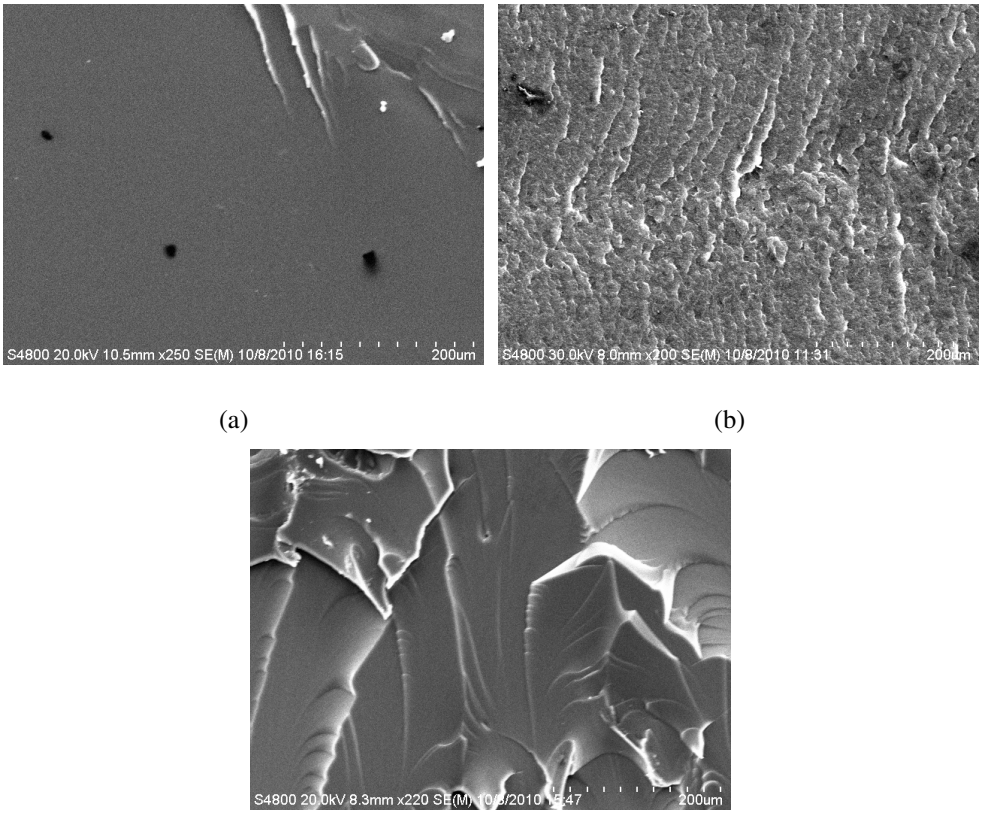

Figure 4.19: Electron microscopy of fractured image of a) DGEB–A resin (b) epoxy/methacryl nanocomposite and (c)epoxy/glycidyl nanocomposite.

Fractured images of DGEB–A resin and their nanocomposites are shown in fig.4.19, that for neat resin surface are smooth while in epoxy/POSS nanocomposite fractured surface are rough, which indicated high dissipation of energy during formation of surface. In case of epoxy/methacryl nanocomposite we can see crack propagation in steps, which indicates arresting of cracks. In case of epoxy/glycidyl nanocomposite surfaces also shows jump of cracks, which indicated toughening of epoxy/POSS nanocomposites by crack pinning mechanism.

4.0.14 Density measurement

Table 4.1 and 4.2 show the density measured by three different ways. It can be observed from values that there is not much variation in density, which is equivalent to the density of neat resin. We can conclude from the tables that incorporation of POSS into resin will not really effect the density of resin (i.e 1.1 g/cc).

	Epoxy/trisilanol phenyl			Epoxy/methacryl			Epoxy/glycidyl		
	ρ_a	ρ_b	ρ_c	ρ_a	ρ_b	ρ_c	ρ_a	ρ_b	ρ_c
0%	1.1	1.1	1.1	1.1	1.1	1.1	1.1	1.1	1.1
0.5%	1	1.1	1.1	1.1	1	1.1	1.1	1.1	1.1
1%	1.1	1.2	1.1	1	1.1	1.1	1.1	1	1.1
3%	1.1	1.1	1.1	1.1	1.1	1.1	1.1	1	1.1
5%	1.1	1.1	1.1	1.1	1.1	1.1	1.1	1	1.1
8%	1.1	1.1	1	1.1	1.1	1.1	1.1	1.1	1.1

Table 4.1: Density measurement of DGEB–F resin and POSS reinforced composites in gm/cc

	Epoxy/methacryl			Epoxy/glycidyl		
	ρ_a	ρ_b	ρ_c	ρ_a	ρ_b	ρ_c
0%	1.1	1.1	1.1	1.1	1.1	1.1
0.5%	1	1.2	1.1	1.1	1	1.1
1%	1.1	1.2	1.1	1	1.1	1.1
3%	1.1	1.1	1.1	1.1	1	1.1
5%	1.1	1.1	1	1.1	1.1	1.1
8%	1	1.1	1	1.1	1.1	1.1

Table 4.2: Density measurement of DGEB-A resin and POSS reinforced composites in gm/cc

CHAPTER 5

CONCLUSIONS and FUTURE WORK

Epoxy/POSS nanocomposites were synthesized and developed by simple technique of mechanical mixing of POSS into epoxy resin. It was observed from the result that with incorporation of POSS into either of the epoxy resins, mechanical and physical properties of nanocomposites vary. Especially in case of DGEB–F resin the effect of POSS is more prominent compared to DGEB–A. With incorporation of POSS, fracture toughness increases up to two times in case of DGEB–F resin and 1.4 times in case of DGEB–A resin, load displacement graph and work of fracture for both resin and their respective nanocomposites also support the fracture toughness result. Glycidyl POSS reinforced nano composites show different behavior compared to epoxy/methacryl and epoxy/trisilanol phenyl nanocomposites in DGEB–F resin. By increasing the loading of glycidyl POSS in resin, failure mode changes from brittle to ductile. This change in failure mode increases the value in the work of fracture and fracture toughness because energy is dissipated in fracturing and plasticization of specimen. While in case of POSS reinforced in DGEB–A resin there is no change in failure mode

While in case of flexural strength and modulus, there was a lot of scattering in data there andmuch difference in the values for both resin. Epoxy/glycidyl nano composite show decrease in value of fracture modulus though.

In order to understand the mechanism going on between POSS and epoxy resins, different characterization techniques like FTIR and DSC were carried out. DSC thermogram

shows that with the addition of POSS in neat resin, glass transition varies depending on the type of interaction between POSS and polymer resin. In case of epoxy/glycidyl and epoxy/methacryl nanocomposites T_g decreases, as functional part of these POSS reacts with polymer chain and increases the free volume. In case of trisilanol phenyl POSS, as POSS only interact with polymer chain restricting the mobility, T_g increses with loading of POSS. This effect of variation of T_g is more prominent in lower fraction of POSS as there is large drop in temperature, while for higher fraction of POSS this decrease is less due to the formation of agglomerates.

BIBLIOGRAPHY

[1] Ellis. B, *Chemistry and technology of epoxy resin*. Blackie academic professional, New York, NY, 1993.

[2] L. In, *Epoxy resin and composites II*. No. 75, Adv. polymer science, Berlin, 1986.

[3] G. M. Kim, H. Qin, X. Fang, F. C. Sun, and P. T. Mather, "Hybrid epoxy-based thermosets based on polyhedral oligosilsesquioxane: Cure behavior and toughening mechanisms," *Journal of polymer science part b-polymer physics*, vol. 41, no. 24, pp. 3299–3313, 2003.

[4] R. PEARSON and A. YEE, "Toughening mechanisms in elastomer-modified epoxies," *journal of materials science*, vol. 24, pp. 2571–2580, JUL 1989.

[5] D. S. PARKER, H. J. SUE, J. HUANG, and A. F. YEE, "Toughening mechanisms in core shell rubber modified polycarbonate," *Polymer*, vol. 31, no. 12, pp. 2267–2277, 1990.

[6] R. Bagheri, M. Williams, and R. Pearson, "Use of surface modified recycled rubber particles for toughening of epoxy polymers," *Polymer Engineering And Science*, vol. 37, pp. 245–251, FEB 1997.

[7] J. Qian, R. Pearson, V. Dimonie, O. Shaffer, and M. ElAasser, "The role of dispersed phase morphology on toughening of epoxies," *Polymer*, vol. 38, pp. 21–30, JAN 1997.

[8] R. Bagheri and R. Pearson, "Role of particle cavitation in rubber-toughened epoxies .1. Microvoid toughening," *Polymer*, vol. 37, pp. 4529–4538, SEP 1996.

[9] J. QIAN, R. PEARSON, V. DIMONIE, and M. ELAASSER, "Synthesis And Application of Core-Shell Particles As Toughening Agents For Epoxies," *Journal Of Applied Polymer Science*, vol. 58, pp. 439–448, OCT 10 1995.

[10] D. W. Y. Wong, L. Lin, P. T. McGrail, T. Peijs, and P. J. Hogg, "Improved fracture toughness of carbon fibre/epoxy composite laminates using dissolvable thermoplastic fibres," *Composites Part A-Applied Science And Manufacturing*, vol. 41, no. 6, pp. 759–767, 2010.

[11] J. K. KIM, C. BAILLIE, J. POH, and Y. W. MAI, "Fracture-toughness of cfrp with modified epoxy-resin matrices," *Composites Science And Technology*, vol. 43, no. 3, pp. 283–297, 1992.

[12] M. Hussain, A. Nakahira, S. Nishijima, and K. Niihara, "Fracture behavior and fracture toughness of particulate filled epoxy composites," *Materials Letters*, vol. 27, no. 1-2, pp. 21–25, 1996.

[13] I. M. LOW, Y. W. MAI, and S. BANDYOPADHAYAY, "Effects of temperature and rate on fracture-toughness of short-alumina-fiber-reinforced epoxies," *Composites Science And Technology*, vol. 43, no. 1, pp. 3–12, 1992.

[14] B. Wetzel, P. Rosso, F. Haupert, and K. Friedrich, "Epoxy nanocomposites - fracture and toughening mechanisms," *Engineering Fracture Mechanics*, vol. 73, pp. 2375–2398, NOV 2006.

[15] S. C. Zunjarrao and R. P. Singh, "Characterization of the fracture behavior of epoxy reinforced with nanometer and micrometer sized aluminum particles," *Composites Science And Technology*, vol. 66, pp. 2296–2305, OCT 2006.

[16] B. Wetzel, F. Haupert, K. Friedrich, M. Zhang, and M. Rong, "Impact and wear resistance of polymer nanocomposites at low filler content," *Polymer Engineering And Science*, vol. 42, pp. 1919–1927, SEP 2002.

[17] R. Singh, M. Zhang, and D. Chan, "Toughening of a brittle thermosetting polymer: Effects of reinforcement particle size and volume fraction," *Journal Of Materials Science*, vol. 37, pp. 781–788, FEB 15 2002.

[18] H. Koerner, E. Hampton, D. Dean, Z. Turgut, L. Drummy, P. Mirau, and R. Vaia, "Generating triaxial reinforced epoxy/montmorillonite nanocomposites with uniaxial magnetic fields," *Chemistry of materials*, vol. 17, no. 8, pp. 1990–1996, 2005.

[19] Q. Chen, I. Chasiotis, C. Chen, and A. Roy, "Nanoscale and effective mechanical behavior and fracture of silica nanocomposites," *Composites Science And Technology*, vol. 68, no. 15-16, pp. 3137–3144, 2008.

[20] B. Qi, Q. X. Zhang, M. Bannister, and Y. W. Mai, "Investigation of the mechanical properties of dgeba-based epoxy resin with nanoclay additives," *Composite Structures*, vol. 75, no. 1-4, pp. 514–519, 2006.

[21] G. Ragosta, M. Abbate, P. Musto, G. Scarinzi, and L. Mascia, "Epoxy-silica particulate nanocomposites: Chemical interactions, reinforcement and fracture toughness," *Polymer*, vol. 46, no. 23, pp. 10506–10516, 2005.

[22] M. Imanaka, Y. Takeuchi, Y. Nakamura, A. Nishimura, and T. Iida, "Fracture toughness of spherical silica-filled epoxy adhesives," *International Journal Of Adhesion And Adhesives*, vol. 21, no. 5, pp. 389–396, 2001.

[23] S. Kang, S. I. Hong, C. R. Choe, M. Park, S. Rim, and J. Kim, "Preparation and characterization of epoxy composites filled with functionalized nanosilica particles obtained via sol-gel process," *Polymer*, vol. 42, no. 3, pp. 879–887, 2001.

[24] Y. Nakamura, S. Okabe, and T. Iida, "Effects of particle shape, size and interfacial adhesion on the fracture strength of silica-filled epoxy resin," *Polymer*, vol. 7, no. 3, pp. 177–186, 1999.

[25] Y. L. Liang and R. A. Pearson, "Toughening mechanisms in epoxy-silica nanocomposites (ESNs)," *Polymer*, vol. 50, pp. 4895–4905, SEP 23 2009.

[26] B. T. Marouf, R. Bagheri, and R. A. Pearson, "Mechanical and thermal properties of montmorillonite-epoxy nanocomposite," *International Journal Of Modern Physics B*, vol. 22, pp. 3247–3253, JUL 30 2008.

[27] S. Zunjarrao, R. Sriraman, and R. Singh, "Effect of processing parameters and clay volume fraction on the mechanical properties of epoxy-clay nanocomposites," *Journal Of Materials Science*, vol. 41, pp. 2219–2228, APR 2006.

[28] R. A. Pearson and Y.-L. Liang, "Toughening mechanisms in epoxy-based hybrid nanocomposites," *Abstracts Of Papers Of The American Chemical Society*, vol. 236, AUG 17 2008.

[29] J. Lee and A. F. Yee, "Fracture behavior of glass bead filled epoxies: Cleaning process of glass beads," *Journal Of Applied Polymer Science*, vol. 79, no. 8, pp. 1371–1383, 2001.

[30] J. Lee and A. F. Yee, "Role of inherent matrix toughness on fracture of glass bead filled epoxies," *POLYMER*, vol. 41, no. 23, pp. 8375–8385, 2000.

[31] A. T. Seyhan, Z. Sun, J. Deitzel, M. Tanoglu, and D. Heider, "Cure kinetics of vapor grown carbon nanofiber (vgcnf) modified epoxy resin suspensions and fracture toughness of their resulting nanocomposites," *Materials Chemistry And Physics*, vol. 118, no. 1, pp. 234–242, 2009.

[32] E. Sancaktar and D. Aussawasathien, "Nanocomposites of epoxy with electrospun carbon nanofibers: Mechanical behavior," *Journal Of Adhesion*, vol. 85, no. 4-5, pp. 160–179, 2009.

[33] Y. X. Zhou, F. Pervin, S. Jeelani, and P. K. Mallick, "Improvement in mechanical properties of carbon fabric-epoxy composite using carbon nanofibers," *Journal Of Materials Processing Technology*, vol. 198, no. 1-3, pp. 445–453, 2008.

[34] S. Maensiri, P. Laokul, J. Klinkaewnarong, and V. Amornkitbamrung, "Carbon nanofiber-reinforced alumina nanocomposites: Fabrication and mechanical properties," *Materials Science And Engineering A-Structural Materials Properties Microstructure And Processing*, vol. 447, no. 1-2, pp. 44–50, 2007.

[35] G. C. Huang, C. H. Lee, and J. K. Lee, "Thermal and mechanical properties of short fiber-reinforced epoxy composites," *Polymer*, vol. 33, no. 6, pp. 530–536, 2009.

[36] Z. Spitalsky, L. Matejka, M. Slouf, E. N. Konyushenko, J. Kovarova, J. Zemek, and J. Kotek, "Modification of carbon nanotubes and its effect on properties of carbon nanotube/epoxy nanocomposites," *Polymer Composites*, vol. 30, no. 10, pp. 1378–1387, 2009.

[37] W. D. Jones, V. K. Rangari, T. A. Hassan, and S. Jeelani, "Synthesis and characterization of (fe3o4/mwcnts)/epoxy nanocomposites," *Journal Of Applied Polymer Science*, vol. 116, no. 5, pp. 2783–2792, 2010.

[38] V. K. Rangari, M. S. Bhuyan, and S. Jeelani, "Microwave processing and characterization of epon 862/cnt nanocomposites," *Materials Science And Engineering B-Advanced Functional Solid-State Materials*, vol. 168, no. 1-3, pp. 117–121, 2010.

[39] M. A. Rafiee, J. Rafiee, Z. Wang, H. H. Song, Z. Z. Yu, and N. Koratkar, "Enhanced mechanical properties of nanocomposites at low graphene content," *Acs Nano*, vol. 3, no. 12, pp. 3884–3890, 2009.

[40] Y. Geng, M. Y. Liu, J. Li, X. M. Shi, and J. K. Kim, "Effects of surfactant treatment on mechanical and electrical properties of cnt/epoxy nanocomposites," *Composites Part A-Applied Science And Manufacturing*, vol. 39, no. 12, pp. 1876–1883, 2008.

[41] T. H. Hsieh, A. J. Kinloch, K. Masania, J. S. Lee, A. C. Taylor, and S. Sprenger, "The toughness of epoxy polymers and fibre composites modified with rubber microparticles and silica nanoparticles," *Journal Of Materials Science*, vol. 45, no. 5, pp. 1193–1210, 2010.

[42] L. Ruiz-Perez, G. J. Royston, J. P. A. Fairclough, and A. J. Ryan, "Toughening by nanostructure," *Polymer*, vol. 49, pp. 4475–4488, OCT 6 2008.

[43] R. M. Hydro and R. A. Pearson, "Epoxies toughened with triblock copolymers," *Journal Of Polymer Science Part B-Polymer Physics*, vol. 45, pp. 1470–1481, JUN 15 2007.

[44] C. H. Ni, G. F. Ni, S. W. Zhang, X. Y. Liu, M. Q. Chen, and L. H. Liu, "The preparation of inorganic/organic hybrid nanomaterials containing silsesquioxane and its reinforcement for an epoxy resin network," *Colloid And Polymer Science*, vol. 288, no. 4, pp. 469–477, 2010.

[45] C. Ramirez, M. Rico, A. Torres, L. Barral, J. Lopez, and B. Montero, "Epoxy/poss organic-inorganic hybrids: Atr-ftir and dsc studies," *EUROPEAN POLYMER JOURNAL*, vol. 44, no. 10, pp. 3035–3045, 2008.

[46] L. Matejka, O. Dukh, B. Meissner, D. Hlavata, J. Brus, and A. Strachota, "Block copolymer organic-inorganic networks. formation and structure ordering," *Macromolecules*, vol. 36, no. 21, pp. 7977–7985, 2003.

[47] R. M. Laine, J. W. Choi, and I. Lee, "Organic-inorganic nanocomposites with completely defined interfacial interactions," *Advanced Materials*, vol. 13, no. 11, pp. 800–+, 2001.

[48] B. S. Hsiao, H. White, M. Rafailovich, P. T. Mather, H. G. Jeon, S. Phillips, J. Lichtenhan, and J. Schwab, "Nanoscale reinforcement of polyhedral oligomeric silsesquioxane (poss) in polyurethane elastomer," *Polymer*, vol. 49, no. 5, pp. 437–440, 2000.

[49] P. T. Mather, H. G. Jeon, A. Romo-Uribe, T. S. Haddad, and J. D. Lichtenhan, "Mechanical relaxation and microstructure of poly(norbornyl-poss) copolymers," *Macromolecules*, vol. 32, no. 4, pp. 1194–1203, 1999.

[50] J. J. Schwab and J. D. Lichtenhan, "Polyhedral oligomeric silsesquioxane (poss)-based polymers," *Applied Organometallic Chemistry*, vol. 12, no. 10-11, pp. 707–713, 1998.

[51] J. D. LICHTENHAN, "Polyhedral oligomeric silsesquioxanes - building-blocks for silsesquioxane-based polymers and hybrid materials," *Comments On Inorganic Chemistry*, vol. 17, no. 2, pp. 115–130, 1995.

[52] K. Wu, L. Song, Y. Hu, H. D. Lu, B. K. Kandola, and E. Kandare, "Synthesis and characterization of a functional polyhedral oligomeric silsesquioxane and its flame retardancy in epoxy resin," *Progress In Organic Coatings*, vol. 65, no. 4, pp. 490–497, 2009.

[53] G. S. Constable, A. J. Lesser, and E. B. Coughlin, "Morphological and mechanical evaluation of hybrid organic-inorganic thermoset copolymers of dicyclopentadiene and mono- or tris(norbornenyl)-substituted polyhedral oligomeric silsesquioxanes," *Macromolecules*, vol. 37, no. 4, pp. 1276–1282, 2004.

[54] K. L. Xie, Y. L. Zhang, and S. Chen, "Synthesis and characterization of reactive polyhedral oligomeric silsesquioxanes (r-poss) containing multi-n-methylol groups," *Journal Of Organometallic Chemistry*, vol. 695, no. 5, pp. 687–691, 2010.

[55] A. Lee and J. D. Lichtenhan, "Viscoelastic responses of polyhedral oligosilsesquioxane reinforced epoxy systems," *Macromolecules*, vol. 31, no. 15, pp. 4970–4974, 1998.

[56] M. Sanchez-Soto, D. A. Schiraldi, and S. Illescas, "Study of the morphology and properties of melt-mixed polycarbonate-poss nanocomposites," *European Polymer Journal*, vol. 45, no. 2, pp. 341–352, 2009.

[57] R. Verker, E. Grossman, I. Gouzman, and N. Eliaz, "Trisilanolphenyl poss-polyimide nanocomposites: Structure-properties relationship," *Composites Science And Technology*, vol. 69, no. 13, pp. 2178–2184, 2009.

[58] A. Strachota, P. Whelan, J. Kriz, J. Brus, M. Urbanova, M. Slouf, and L. Matejka, "Formation of nanostructured epoxy networks containing polyhedral oligomeric silsesquioxane (poss) blocks," *Polymer*, vol. 48, no. 11, pp. 3041–3058, 2007.

[59] E. T. Kopesky, G. H. McKinley, and R. E. Cohen, "Toughened poly(methyl methacrylate) nanocomposites by incorporating polyhedral oligomeric silsesquioxanes," *Polymer*, vol. 47, no. 1, pp. 299–309, 2006.

[60] L. Matejka, A. Strachota, J. Plestil, P. Whelan, M. Steinhart, and M. Slouf, "Epoxy networks reinforced with polyhedral oligomeric silsesquioxanes (poss). structure and morphology," *Macromolecules*, vol. 37, no. 25, pp. 9449–9456, 2004.

[61] F. Zhao, X. J. Bao, A. R. McLauchlin, J. J. Gu, C. Y. Wan, and B. Kandasubramanian, "Effect of poss on morphology and mechanical properties of polyamide 12/montmorillonite nanocomposites," *Applied Clay Science*, vol. 47, no. 3-4, pp. 249–256, 2010.

[62] L. Song, Q. L. He, Y. Hu, H. Chen, and L. Liu, "Study on thermal degradation and combustion behaviors of pc/poss hybrids," *Polymer Degradation And Stability*, vol. 93, no. 3, pp. 627–639, 2008.

[63] Y. D. Zhang, S. H. Lee, M. Yoonessi, K. W. Liang, and C. U. Pittman, "Phenolic resin-trisilanolphenyl polyhedral oligorneric silsesquioxane (poss) hybrid nanocomposites: Structure and properties," *Polymer*, vol. 47, no. 9, pp. 2984–2996, 2006.

[64] J. J. Zeng, C. Bennett, W. L. Jarrett, S. Iyer, S. Kumar, L. J. Mathias, and D. A. Schiraldi, "Structural changes in trisilanol poss during nanocomposite melt processing," *Composite Interfaces*, vol. 11, no. 8-9, pp. 673–685, 2005.

[65] S. Iyer and D. A. Schiraldi, "Role of specific interactions and solubility in the reinforcement of bisphenol a polymers with polyhedral oligomeric silsesquioxanes," *Macromolecules*, vol. 40, no. 14, pp. 4942–4952, 2007.

[66] J. Liu, Z. J. Thompson, H. J. Sue, F. S. Bates, M. A. Hillmyer, M. Dettloff, G. Jacob, N. Verghese, and H. Pham, "Toughening of epoxies with block copolymer micelles of wormlike morphology," *Macromolecules*, vol. 43, no. 17, pp. 7238–7243, 2010.

[67] A. Buchman, H. Dodiuk-Kenig, A. Dotan, R. Tenne, and S. Kenig, "Toughening of epoxy adhesives by nanoparticles," *Journal Of Adhesion Science And Technology*, vol. 23, no. 5, pp. 753–768, 2009.

[68] F. J. Feher, S. Luecke, J. J. Schwab, J. D. Lichtenhan, S. H. Phillips, and A. Lee, "Hybrid materials from epoxide-substituted poss frameworks.," *Abstracts Of Papers Of The American Chemical Society*, vol. 219, 2000.

[69] A. Lee, J. D. Lichtenhan, and W. A. Reinerth, "Epoxy-poss and epoxy-clay nanocomposites: Thermal and viscoelastic comparison.," *Abstracts Of Papers Of The American Chemical Society*, vol. 219, 2000.

[70] J. J. Schwab, J. D. Lichtenhan, K. P. Chaffee, J. C. Gordon, Y. A. Otonari, M. J. Carr, and A. G. Bolf, "Investigations into structure/property relationships for polyhedral oligomeric silsesquioxane (poss) based methacrylate polymers," *Abstracts Of Papers Of The American Chemical Society*, vol. 213, pp. 351–POLY, 1997.

[71] J. Fu, L. Y. Shi, Y. Chen, S. Yuan, J. Wu, X. L. Liang, and Q. D. Zhong, "Epoxy nanocomposites containing mercaptopropyl polyhedral oligomeric silsesquioxane:

Morphology, thermal properties, and toughening mechanism," *Journal Of Applied Polymer Science*, vol. 109, no. 1, pp. 340–349, 2008.

[72] M. Spirkova, A. Strachota, L. Brozova, J. Brus, M. Urbanova, J. Baldrian, M. Slouf, O. Blahova, and P. Duchek, "The influence of nanoadditives on surface, permeability and mechanical properties of self-organized organic-inorganic nanocomposite coatings," *Journal Of Coatings Technology And Research*, vol. 7, no. 2, pp. 219–228, 2010.

[73] "www.appliedpoleramics.com."

[74] "www.hexion.com."

[75] "www.hybridplastics.com."

[76] A. TL, *Fracture mechanics: fundamentals and applications.* Boca Rotan (FL), CRC Press, 1991.

[77] American society for testing and materials., Philadelphia, PA, *ASTM D5045-99: Standard test methods for plain-strain fracture toughness and strain energy release rate of plastic materials.*, 1999.

[78] American society for testing and materials., Philadelphia, PA, *ASTM D790-07: Standard test methods for flexural properties of unreinforced and reinforced palstics and electrical insulating materials.*

VITA

Kunal Mishra

Candidate for the Degree of

Candidate for the Degree of Master of Science

Thesis: A STUDY ON DEVELOPING OF EPOXY/POSS NANOCOMPOSITE AND TO INVESTIGATE THEIR THERMO–MECHANICAL BEHAVIOR

Major Field: Mechanical Engineering

Biographical:

Personal Data: Born in Gurgaon, Haryana, India on May 15th 1983.

Education:

Received the B.Tech. degree from Uttar pradesh technical university,Lucknow, Uttar Pradesh, India, 2008, in Mechanical Engineering
Completed the requirements for the degree of Master of Science with a major in Mechanical Engineering Oklahoma State University in May, 2011.

Experience:

Worked as a Graduate Research Assistant at the Mechanics of Advanced Materials Laboratory headed by Dr. Raman P. Singh in the area of reinforced nanocomposites

Name: Kunal Mishra Date of Degree: May, 2011

Institution: Oklahoma State University Location: Stillwater, Oklahoma

Title of Study: A STUDY ON DEVELOPING OF EPOXY/POSS NANOCOMPOSITE AND TO INVESTIGATE THEIR THERMO–MECHANICAL BEHAVIOR

Pages in Study: 47 Candidate for the Degree of Master of Science

Major Field: Mechanical and Aerospace Engineering

This study reports on the developing of epoxy/POSS nanocomposites and to investigate their thermo-mechanical behavior. Three distinct types of POSS, with trisilanol phenyl, methacryl and glycidyl functionalities are used as reinforcement of DGEB–F and DGEB–A based resin, cured using an amine based hardener. The POSS is added at low weight fraction of 0.5%, 1%, 3%, 5% and 8% by direct mechanical mixing. The mechanical properties of resin are characterized in terms of fracture toughness (critical stress intensity factor, K_{Ic}), Work of fracture (J/m^2) flexural strength (MPa) and modulus of elasticity (GPa). It is found that with increase of POSS loading the fracture toughness increases for all type of functionality. For DGEB–F based nanocomposites it increases upto 120% and with DGEB–A based resin it increase upto 40%. The value of flexural strength and modulus of elasticity was not different considering the large scattering of data. It has been found from the results of mechanical properties that POSS with greater interaction with polymer resin shows better result. The interaction between functional group of POSS and epoxy resin was showed Fourier transformation infra- red (FTIR). The differential scanning calorimetry (DSC) showed that reinforcing the POSS cause decrease in composite's T_g however being relatively greater importance for low POSS contents. The resulting fracture surface morphology were examined using scanning electron microscopy (SEM). Fractographic observation shows rougher surface for POSS reinforced resin (both DGEB–F and DGEB–A) that further indicates the evidence of extrinsic toughening mechanisms. Higher magnification of fractured surface of epoxy/POSS nanocomposites shows formation of agglomeration at high percentage of POSS loading as formation of voids and microcracks was observed. Density of neat resin and epoxy/POSS nanocomposites was measured by three different ways. Result shows that value of densities was not varying much by incorporation of POSS in resin.

ADVISOR'S APPROVAL: _____